BIOMOLECULES & THERAPEUTICS

Original Article
Biomol Ther 31(1), 127-138 (2023)

Virtual Screening and Testing of GSK-3 Inhibitors Using Human SH-SY5Y Cells Expressing Tau Folding Reporter and Mouse Hippocampal Primary Culture under Tau Cytotoxicity

Chih-Hsin Lin[1,†], Yu-Shao Hsieh[2,†], Ying-Chieh Sun[2,†], Wun-Han Huang[1], Shu-Ling Chen[1], Zheng-Kui Weng[1], Te-Hsien Lin[1], Yih-Ru Wu[3], Kuo-Hsuan Chang[3], Hei-Jen Huang[4], Guan-Chiun Lee[1,*], Hsiu Mei Hsieh-Li[1,*] and Guey-Jen Lee-Chen[1,*]

[1]School of Life Science, National Taiwan Normal University, Taipei 11677,
[2]Department of Chemistry, National Taiwan Normal University, Taipei 11677,
[3]Department of Neurology, Chang Gung Memorial Hospital, Taoyuan 33378,
[4]Department of Nursing, Mackay Junior College of Medicine, Nursing and Management, Taipei 11260, Taiwan

Abstract

Glycogen synthase kinase-3β (GSK-3β) is an important serine/threonine kinase that implicates in multiple cellular processes and links with the neurodegenerative diseases including Alzheimer's disease (AD). In this study, structure-based virtual screening was performed to search database for compounds targeting GSK-3β from Enamine's screening collection. Of the top-ranked compounds, 7 primary hits underwent a luminescent kinase assay and a cell assay using human neuroblastoma SH-SY5Y cells expressing Tau repeat domain (Tau_{RD}) with pro-aggregant mutation ΔK280. In the kinase assay for these 7 compounds, residual GSK-3β activities ranged from 36.1% to 90.0% were detected at the IC_{50} of SB-216763. In the cell assay, only compounds VB-030 and VB-037 reduced Tau aggregation in SH-SY5Y cells expressing ΔK280 Tau_{RD}-DsRed folding reporter. In SH-SY5Y cells expressing ΔK280 Tau_{RD}, neither VB-030 nor VB-037 increased expression of GSK-3α Ser21 or GSK-3β Ser9. Among extracellular signal-regulated kinase (ERK), AKT serine/threonine kinase 1 (AKT), mitogen-activated protein kinase 14 (P38) and mitogen-activated protein kinase 8 (JNK) which modulate Tau phosphorylation, VB-037 attenuated active phosphorylation of P38 Thr180/Tyr182, whereas VB-030 had no effect on the phosphorylation status of ERK, AKT, P38 or JNK. However, both VB-030 and VB-037 reduced endogenous Tau phosphorylation at Ser202, Thr231, Ser396 and Ser404 in neuronally differentiated SH-SY5Y expressing ΔK280 Tau_{RD}. In addition, VB-030 and VB-037 further improved neuronal survival and/or neurite length and branch in mouse hippocampal primary culture under Tau cytotoxicity. Overall, through inhibiting GSK-3β kinase activity and/or p-P38 (Thr180/Tyr182), both compounds may serve as promising candidates to reduce Tau aggregation/cytotoxicity for AD treatment.

Key Words: GSK-3β kinase inhibitor, Alzheimer's disease, Virtual screening, Enzyme assay, Cell assay, Mouse hippocampal primary culture

INTRODUCTION

Alzheimer's disease (AD) is the most common neurodegenerative disorder accompanied with progressive memory loss and cognitive impairment. The neuropathological diagnosis of AD relies on the presence of amyloid plaques and *neurofibrillary tangles* (NFTs) (Hardy, 2006). Glycogen synthase kinase-3β (GSK-3β) is an evolutionarily conserved serine/

Open Access **https://doi.org/10.4062/biomolther.2022.035**

Received Mar 11, 2022 **Revised** May 5, 2022 **Accepted** May 24, 2022
Published Online Jul 5, 2022

***Corresponding Authors**
E-mail: gclee@ntnu.edu.tw (Lee GC),
hmhsieh@ntnu.edu.tw (Hsieh-Li HM),
t43019@ntnu.edu.tw (Lee-Chen GJ)
Tel:+886-2-7749-6351 (Lee GC), +886-2-7749-6354 (Hsieh-Li HM),
+886-2-7749-6359 (Lee-Chen GJ)
Fax:+886-2-2931-2904 (Lee GC), +886-2-2931-2904 (Hsieh-Li HM),
+886-2-2931-2904 (Lee-Chen GJ)
[†]The first three authors contributed equally to this work.

threonine kinase that phosphorylates cellular substrates and thereby regulates diverse cellular functions, including cellular signaling (Grimes and Jope, 2001) and apoptosis (Li *et al*., 2000). It has been shown that GSK-3β is a crucial contributor to Tau phosphorylation (Lee *et al*., 2003) and also has been proposed to contribute to amyloid production (Su *et al*., 2004). In AD brains, GSK-3β is co-localized with neurofibrillary changes, with increased levels in post-synaptosomal supernatant as compared to the controls (Pei *et al*., 1997). Overexpression of GSK-3β in adult mouse brain results in hyperphosphorylation of Tau in hippocampal neurons and neurodegeneration (Lucas *et al*., 2001). Inhibition of GSK-3β by BTA-EG_4, an amyloid-binding drug which reduces Aβ-induced toxicity *in vitro* (Inbar *et al*., 2006), reduces Tau phosphorylation in brain slice cultures from 3×Tg-AD mice (Croft *et al*., 2017). Therefore, identification of effective GSK-3β inhibitors modulating aberrant Tau phosphorylation serves as an attractive therapeutic strategy for AD.

There are two isoforms of GSK-3, GSK-3α (51 kDa) and GSK-3β (47 kDa), encoded by separate genes, which share extensive similarities in their catalytic domains, but differ in their N- and C-terminal regions (Woodgett, 1990). Unlike other protein kinases, GSK-3 is constitutively active and is inactivated by upstream regulators in response to stimuli. Several signaling pathways regulate GSK-3 activity (Hur and Zhou, 2010). Activation of the phosphatidylinositol 3-kinase (PI3K)-AKT serine/threonine kinase 1 (AKT) pathway results in inactivation of GSK-3 through phosphorylation at N-terminal Ser9 (GSK-3β) or Ser21 (GSK-3α) (Cross *et al*., 1995). Inhibitory phosphorylation of GSK-3β at Ser9 can also be achieved through protein kinase C (PKC)-α-induced extracellular signal-regulated kinase (ERK) and mitogen-activated protein kinase 14 (P38) pathways to attenuate Tau phosphorylation at Ser396 (Nemoto *et al*., 2010). In addition to GSK-3β, Tau phosphorylation can also be mediated by P38 (Lauretti and Praticò, 2015) and mitogen-activated protein kinase 8 (JNK) (Ploia *et al*., 2011).

Over the past decade, various classes of small molecule GSK-3β inhibitors with diverse mechanisms have been reported for the treatment of AD. Lithium, a natural, inorganic and water-soluble GSK-3β inhibitor, reduces Tau phosphorylation and insoluble Tau levels in transgenic mice overexpressing human P301L mutant Tau (Noble *et al*., 2005). Although upregulation of brain derived neurotrophic factor might be part of a neuroprotective effect of lithium in AD patients (Leyhe *et al*., 2009), no treatment effect on GSK-3 activity or cerebrospinal fluid-based biomarker concentrations was observed in lithium trial in AD (Hampel *et al*., 2009). Another GSK-3β inhibitor, tideglusib, showed safety and efficacy demonstrated in a small pilot study (del Ser *et al*., 2013). However, a short term (26 weeks) phase II trial of tideglusib produced no clinical benefit in AD (Lovestone *et al*., 2015). Furthermore, for arylindolemaleimides SB-216763 and SB-415286 that inhibit GSK-3 *in vitro*, a previous study demonstrated that these compounds promote survival of primary neurons following the survival factor withdrawal or inhibition of PI3K activity (Cross *et al*., 2001). Although both SB inhibitors strongly facilitate regrowth of cerebellar granule neurons and improve axon regeneration in injured cortical neurons (Seira *et al*., 2010), SB-216763 inhibited neurite growth in cerebellar and dorsal root ganglion neurons (Alabed *et al*., 2010). With these collective current results of GSK-3 inhibition, nevertheless, GSK-3 could be considered as a target for modulating production and integration of new neurons in hippocampus as a treatment for neurodegenerative diseases (Eldar-Finkelman and Martinez, 2011). Therefore, identification of new lead GSK-3β inhibitors for treating AD continues to spur considerable interest (Shi *et al*., 2020).

In this study, virtual screening using the docking computation combined with a compound structure similarity search was first utilized to screen compounds in a database in order to identify novel GSK-3β inhibitors. Among the top-ranked compounds, seven compounds were selected and underwent *in vitro* GSK-3β inhibition and cell-based assays to examine their inhibition strengths and their effects on Tau aggregation. In addition, neuroprotection effect on primary hippocampal neuronal culture was also investigated.

MATERIALS AND METHODS

Virtual screening

The GOLD docking program (Verdonk *et al*., 2003) was used to screen 1.5 million compounds collected from the Enamine database (http://www.enamine.net/). Details of computational protocol have been described in our previous work (Lin *et al*., 2016). Briefly, the docking protocol for virtual screening was selected among several tested protocols based on the performance of the associated benchmark tests, including selection of protein crystal structures and hydrogen-bond (H-bond) constraints which enhanced screening results for docking ligands against kinases (Perola, 2006). This protocol optimization process yielded the final protocol for virtual screening. The GSK-3β structure in the GSK-3β-ligand crystal structure (PDB code 2OW3) (Zhang *et al*., 2007) was used for docking. The protocol of protein H-bond constraints was used, and the C=O of Asp133 and N-H of Val135 in the hinge-region of the ATP-binding site were selected as H-bond formation sites such that compounds forming these finger print H-bonds will be biased and favored. The ChemScore scoring function was used to estimate interaction strength between ligands and GSK-3β. A total of 16 compounds from virtual screening were suggested to undergo experimental tests. The computed binding strengths of these compounds are listed in Supplementary Table 1. Among these suggested top-ranked compounds, seven were selected (Fig. 1) due to budget consideration and availability, and obtained from Enamine (Kiev, Ukraine) for enzyme, cell, and mouse hippocampal primary neuron culture tests. The remaining 9 compounds are shown in Supplementary Fig. 1. The selected 7 compounds (Enamine's ID) were: VB-030 (Z1157726443), 031 (Z1157726458), 032 (Z56849949), 035 (Z773887392), 036 (Z46527339), 037 (Z46595412) and 041 (Z29017365). According to IUPAC nomenclature, the structures of quinoline compounds VB-030 and VB-037 are 2-(pyridin-4-yl)-4-(p-tolyl)quinoline and (E)-4-(3-(2-(5-nitroquinolin-2-yl)vinyl)quinolin-2-yl)morpholine, respectively.

Bioavailability and BBB permeation prediction

Molecular weight, H-bond donor, H-bond acceptor, octanol-water partition coefficient, and polar surface area of VB compounds were calculated using Internet software ChemDraw (http://www.perkinelmer.com/tw/category/chemdraw/). In addition, BBB permeation scores were computed using an online BBB prediction server (https://www.cbligand.org/BBB/).

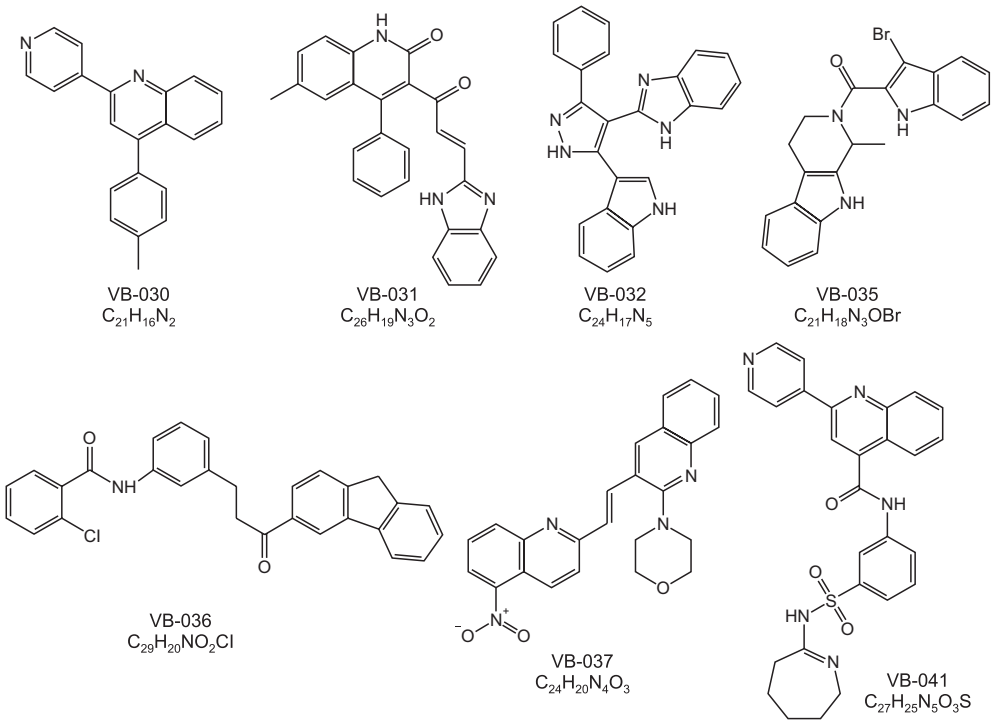

Fig. 1. Structures and formulas of the seven selected VB-030, -031, -032, -035, -036, -037 and -041 obtained from virtual screening of the Enamine database.

GSK-3β kinase assay

The ability of the seven selected VB compounds to inhibit GSK-3β kinase was evaluated, wherein a known GSK-3β inhibitor SB-216763 (Sigma-Aldrich, St Louis, MO, USA) served as a positive control. GSK-3β kinase activity was measured in the presence of test compounds using GSK-3β Kinase Enzyme System (Promega, Madison, WI, USA). Reactions were performed at 30°C for 30 minutes in the 25 μL mixture containing 25 μM ATP, 0.2 mg/mL GSK-3β substrate, 1 ng GSK-3β, and 0.018 μM SB-216763 (44) or VB compounds. Kinase activity data were measured as relative light units (RLU) directly correlated with the amount of ADP produced by using SpectraMax L microplate reader (Molecular Devices, Sunnyvale, CA, USA).

Tet-on ΔK280 Tau_{RD}-DsRed SH-SY5Y cells and fluorescence intensity analysis

Human SH-SY5Y cells expressing DsRed tagged pro-aggregated mutant (ΔK280) of C-terminal repeat domain of Tau (Tau_{RD}, Gln^{244}-Glu^{372} of the longest Tau^{441} isoform) (Lin *et al.*, 2016) were maintained in medium containing 5 μg/mL blasticidin and 100 μg/mL hygromycin (Invitrogen, Carlsbad, CA, USA). On day 1, cells were seeded into 96-well (2×10^4/well) plates with retinoic acid (10 μM; Sigma-Aldrich) added to induce neuronal differentiation. On day 2, the cells were pretreated with test VB compounds (2-10 μM) for 8 h, followed by turning on the hybrid human cytomegalovirus (CMV)/$TetO_2$ promoter-driving ΔK280 Tau_{RD}-DsRed expression with doxycycline (2 μg/mL; Sigma-Aldrich). The cells were kept in the medium containing retinoic acid, doxycycline and test VB compounds for 6 days. In addition, congo red and SB-415286 (2-10 μM; Sigma-Aldrich) were included for comparison. On day 8, cells were stained with Hoechst 33342 (0.1 μg/mL; Sigma-Aldrich), cell images were automatically recorded at 531/40 nm excitation and 593/40 nm emission wavelengths (ImageXpress Micro Confocal High-Content Imaging System, Molecular Devices) and analyzed (MetaXpress High-Content Image Acquisition and Analysis Software, Molecular Devices). EC_{50} (half maximal effective concentration) was estimated by a method of interpolation.

Cell proliferation assay

To evaluate compound cytotoxicity, 2×10^4 ΔK280 Tau_{RD}-DsRed SH-SY5Y cells were plated on 96-well dishes with retinoic acid (10 μM) on day 1. On day 2, the cells were treated with the test compounds (1-100 μM) for 8 h, followed by inducing ΔK280 Tau_{RD}-DsRed expression with doxycycline (2 μg/mL). On day 8, 10 μL of 3-(4,5-dimethylthiazol-2-yl)-2,5-diphenyltetrazolium bromide (MTT) (5 mg/mL) was added to the cells at 37°C for 3 h. 100 μL of lysis buffer (10% Triton X-100, 0.1 N HCl, 18% isopropanol) was then added to dishes and the absorbance of the insoluble purple formazan product at OD 570 nm was read by a FLx800 fluorescence microplate spectrophotometer (Bio-Tek, Winooski, VT, USA). IC_{50} (half maximal inhibitory concentration) was estimated by a method of interpolation.

Real-time quantitative reverse transcription PCR analysis

ΔK280 Tau_{RD}-DsRed SH-SY5Y cells were seeded in a 6-well plate (5×10^5/well), differentiated with retinoic acid, and treated with congo red, SB-415286, VB-030 or VB-037 (10 μM) and doxycycline as described. On day 8, cells were collected and total RNA was extracted using Trizol reagent (Invitrogen). The RNA was reverse-transcribed using high-ca-

pacity cDNA reverse transcriptase (Thermo Fisher Scientific, Waltham, MA, USA). Real-time quantitative PCR experiments were performed using 100 ng cDNA and customized Assays-by-Design probe for DsRed and HPRT1 (4326321E) using StepOnePlus Real-time PCR system (Applied Biosystems, Foster City, CA, USA). Fold change was calculated using the formula $2^{\Delta Ct}$, $\Delta C_T = C_T$ (HPRT1)–C_T (DsRed), in which C_T indicates cycle threshold.

Western blot analysis

As described, ΔK280 Tau_{RD}-DsRed SH-SY5Y cells were seeded in a 6-well plate and treated with retinoic acid, test compounds (10 μM) and doxycycline. On day 8, cells were collected and total proteins were prepared using lysis buffer containing 10 mM Tris-HCl pH 7.5, 150 mM NaCl, 5 mM EDTA, pH 8.0, 0.1% SDS, 1% sodium deoxycholate, 1% NP-40, as well as protease (Sigma-Aldrich) and phosphatase (Abcam, Cambridge, MA, USA) inhibitor cocktails. Proteins (25 μg) were separated on 10% SDS-polyacrylamide gel electrophoresis and transferred onto polyvinylidene difluoride membranes (Sigma-Aldrich) by reverse electrophoresis. After blocking, the membrane was probed with DsRed (1:500; Santa Cruz Biotechnology, Dallas, TX, USA), GSK-3α and GSK-3β (1:500; Santa Cruz Biotechnology), p-GSK-3α (S21) (1:1000; Cell Signaling Technology, Beverly, MA, USA), p-GSK-3β (S9) (1:1000; Cell Signaling Technology), ERK and p-ERK (T202/Y204) (1:1000; Cell Signaling Technology), AKT and p-AKT (S473) (1:2000; Cell Signaling Technology), P38 and p-P38 (T180/Y182) (1:1000; Cell Signaling Technology), JNK and p-JNK (T183/Y185) (1:2000; Cell Signaling Technology), Tau (1:500; Dako, Glostrup, Denmark), p-Tau (S202) (1:2000; AnaSpec Inc., Fremont, CA, USA), p-Tau (T231 and S404) (1:2000; Sigma-Aldrich), p-Tau (S396) (1:1000; Sigma-Aldrich), and GAPDH (1:2000; MDBio Inc., Taipei, Taiwan) at 4°C overnight. After extensive washing, the immune complexes were detected by horseradish peroxidase-conjugated goat anti-mouse or goat anti-rabbit IgG antibody (1:5000; GeneTex, Irvine, CA, USA) and chemiluminescence substrate (Millipore, Billerica, MA, USA).

Compound treatment on primary hippocampal neuronal culture

All experiments were performed according to the guidelines of the Institutional Animal Care and Use Committee of National Taiwan Normal University, Taipei, Taiwan. Female pregnant mice (C57BL/6J) were purchased from the National Breeding Centre for Laboratory Animals (Taipei, Taiwan). Mouse hippocampi were isolated from embryonic brains on days 16°C18 and trypsinized (0.05%) for 15 min in 37°C and cells were cultured in neurobasal plating media as described). Briefly, the hippocampal cells were plated into poly-L-lysine (100 μg/mL)-pretreated flasks (48-well plates; 3×10^4 cells per culture well). The cultures were incubated in a tissue culture incubator at 37°C in 5% CO_2. On days *in vitro* (DIV) 1, 4 and 7, half of the culture media was replaced with fresh media without horse serum. On DIV 4 and 7, cytosine arabinoside (2 μM) was added to the culture to reduce the glial cell populations, which the hippocampal neuronal population was enriched. On DIV 9, the cells were treated with 10 nM wortmannin and GF109203X to induce Tau hyperphosphorylation to mimic the AD pathological condition (Liu *et al*., 2003; Xu *et al*., 2005). VB-030 or VB-037 (1 μM) was added to the cells sequentially. Cells were harvested 12 h later for immunocytochemical staining.

Immunocytochemical staining of hippocampal primary culture

The neuronal survival and morphology of the hippocampal primary culture were evaluated by immunocytochemical staining with antibodies against NeuN (neuron-specific RNA binding nuclear protein) and Map2 (microtubule-associated protein 2, for neurite morphology). Cells were fixed and stained with primary antibodies (1:1000; NeuN and Map2; Millipore) and then fluorescence tagged secondary antibodies and 4',6-diamidino-2-phenylindole (DAPI) for nuclei. Mature neuron, neurite length and branching were analyzed by Metamorph image analysis software (ImageXpress Micro, Molecular Devices) using images from evenly distributed 16 arenas in each well (totally 64 arenas was set) from independent three experiments. Each neurite length longer than 2 folds of neuronal soma diameter was included.

Statistical analysis

For each set of values, data were expressed as the mean ± standard deviation (SD). Three independent tests in two or three biological replicates were performed in each experiment and differences between groups were evaluated by Student's *t*-test or one-way analysis of variance (ANOVA) with *post-hoc* Tukey test, where appropriate. Statistical significance was set at $p<0.05$.

RESULTS

Selected top-ranked compounds from virtual screening and prediction of bioavailability and BBB permeation

A large number of structurally diverse potent GSK-3β inhibitors have been reported (Xu *et al*., 2019). In pursuit of finding potent GSK-3β inhibitors for the treatment of AD, we combined docking calculations and similarity searches to perform structure-based virtual screening. Supplementary Fig. 2 displays GSK-3β structure used for docking and the finger print H-bond interactions between the hinge-region of the ATP-binding site and compounds. Structures and formulas of the selected seven top-ranked VB compounds (030, 031, 032, 035, 036, 037 and 041) are shown in Fig. 1. Based on molecular weight (MW), hydrogen bond donors (HBD), hydrogen bond acceptors (HBA), and calculated octanol/water partition coefficient (cLogP), most VB compounds meet Lipinski's rule of 5 guidelines for predicting oral bioavailability (MW≤450, HBD ≤5, HBA≤10, cLogP≤5) (Lipinski *et al*., 2001) (Table 1). With a polar surface area (PSA) less than 90 $Å^2$, compounds except VB-041 were predicted to diffuse across the blood-brain barrier (BBB) (Hitchcock and Pennington, 2006), as also suggested by online BBB predictor (BBB permeation score greater than the threshold 0.02) (Liu *et al*., 2014) (Table 1).

Test of GSK-3β inhibition

In vitro GSK-3β inhibition assay was used to examine the inhibition strengths of these VB compounds. When the concentrations of these VB compounds were set at 0.018 μM, the IC_{50} of SB-216763 at 25 μM ATP (Lin *et al*., 2016), the detected residual activities of GSK-3β were shown in Table 2. Under the reaction conditions of this study, the VB compound concentration of 0.018 μM did not form colloidal aggregates,

Table 1. Prediction of bioavailability and BBB permeation

Compound	VB-030	VB-031	VB-032	VB-035	VB-036	VB-037	VB-041
MW	296.4	405.4	375.4	408.3	449.9	412.4	499.6
HBD	0	2	3	2	1	0	2
HBA	2	5	5	4	3	7	8
cLogP	5.1	4.6	5.0	5.0	6.1	4.5	3.4
PSA (Å^2)	25	71	61	44	46	89	112
BBB score	0.341	0.095	0.193	0.237	0.181	0.096	0.060

MW, molecular weight; HBD, hydrogen bond donor; HBA, hydrogen bond acceptor; cLogP, calculated octanol-water partition coefficient; PSA, polar surface area; BBB, blood-brain barrier.

Table 2. Inhibition potency against GSK-3β kinase

Compound	VB-030	VB-031	VB-032	VB-035	VB-036	VB-037	VB-041
Residual GSK-3β activity at 0.018 μM (%)	36.1 ± 1.1	63.1 ± 1.2	82.0 ± 8.8	79.9 ± 3.8	75.2 ± 4.8	90.9 ± 6.6	79.2 ± 6.2

SB-216763 was used as a positive inhibitor control for GSK-3β activity assay which gave an IC_{50} of 0.018 μM. The data were obtained from three independent experiments (n=3).

and thus non-specific enzyme-aggregate inhibition could be ruled out. The lower residual GSK-3β activity indicates stronger inhibitory ability of the compound. Among these VB compounds, VB-030 was the most potent in inhibiting GSK-3β (36.1 ± 1.1% residual GSK-3β activity at 0.018 μM), whereas VB-037 was the least potent in inhibiting GSK-3β (90.9 ± 6.6% residual GSK-3β activity at 0.018 μM).

Test of VB compounds reducing tau aggregation in ΔK280 Tau_{RD}-DsRed-expressing SH-SY5Y cells

Tet-On ΔK280 Tau_{RD}-DsRed SH-SY5Y cells with DsRed fluorescence reflecting Tau aggregation status (Lin *et al*., 2016) were used to examine the ability of VB compounds to reduce ΔK280 Tau_{RD} aggregation and promote Tau-DsRed solubility. Congo red and SB-415286 known to reduce Tau aggregates in HEK293 cells (Lin *et al*., 2016) were included for comparison. The poorly folded ΔK280 Tau_{RD} formed aggregates to adversely affect the folding of fused DsRed and thus decrease DsRed fluorescence. The retinoic acid-differentiated SH-SY5Y cells were pretreated with different concentrations of test compounds (2-10 μM) for 8 h, followed by inducing ΔK280 Tau_{RD}-DsRed expression with doxycycline for 6 days (Fig. 2A). As shown in Fig. 2B, treatment with congo red at 5-10 μM (109-118%, p=0.010-0.001), SB-415286 at 10 μM (110%, p=0.008), VB-030 at 10 μM (109%, p=0.010) or VB-037 at 5-10 μM (113-130%, p=0.006-0.002) increased the DsRed fluorescence intensity significantly compared with untreated cells (100%). As a measure of Tau aggregation inhibition, congo red, SB-415286, VB-030 and VB-037 had EC_{50} values of 32.9, 47.5, 54.9 and 15.5 μM, respectively (Supplementary Fig. 3A). Greater than 77% of cell viability was observed following treatment with congo red, SB-415286, VB-030 or VB-037 at 10 μM concentration. Based on the cell number analyzed, the IC_{50} cytotoxicity values of congo red, SB-415286, VB-030 and VB-037 in SH-SY5Y cells expressing ΔK280 Tau_{RD}-DsRed for 6 days were all greater than 10 μM. Representative DsRed fluorescent images of ΔK280 Tau_{RD}-expressing cells untreated or treated with congo red, SB-415286, VB-030 or VB-037 (10 μM) are shown in Fig. 2C. When cell viability assay was performed following treatment with 2-50 μM congo red, SB-415286, VB-030 and VB-037, IC_{50} values were 54.8, 53.2, 44.8 and 66.5 μM, respectively (Fig. 2D, Supplementary Fig. 3B). Addition of 10 μM congo red, SB-415286, VB-030 or VB-037 did not alter the relative ΔK280 Tau_{RD}-DsRed/HPRT1 RNA level as determined by real-time quantitative reverse transcription PCR (24.3-25.2 vs. 24.2 folds of induction; p>0.05) (Fig. 2E). Significantly increased soluble ΔK280 Tau_{RD}-DsRed protein was also observed in cells treated with congo red, SB-415286, VB-030 or VB-037 (117-129%, p=0.021-<0.001) compared with untreated cells (100%) (Fig. 2F).

Tests of VB-030 and VB-037 on inhibiting Tau phosphorylation

We then examined the effect of SB-415286, VB-030 and VB-037 on the levels of p-GSK-3α at Ser21 (to inactivate GSK-3α) and p-GSK-3β at Ser9 (to inactivate GSK-3β) (Fig. 3A) in ΔK280 Tau_{RD}-DsRed-expressing SH-SY5Y cells by Western blotting. No significant difference was detected in the level of total GSK-3α (92-99% versus 100%, p>0.05) or GSK-3β (107-110% versus 100%, p>0.05) protein between test compound-treated and untreated control. As a positive control, a significant increase in the level of p-GSK-3α (Ser21) (150% versus 105%, p=0.002) and p-GSK-3β (Ser9) (133% versus 105%, p=0.023) was observed in SB-415286-treated cells compared with untreated control. However, neither VB-030 nor VB-037 increased expression of GSK-3α Ser21 (103-112%) or GSK-3β Ser9 (102-106%) (p>0.05).

The effects of SB-415286, VB-030 and VB-037 on the levels of kinases which phosphorylate Tau including ERK, AKT, P38 and JNK were then examined (Fig. 3B). Treatment of SB-415286 increased the level of p-ERK (Thr202/Tyr204) (135% versus 103%, p=0.013) and p-AKT (Ser473) (130% versus 96%, p=0.012), while treatment of VB-037 decreased the level of p-P38 (Thr180/Tyr182) (47% versus 77%, p=0.047). Again, no significant difference was detected in the levels of total ERK (91–101%), AKT (97–103%), P38 (88–97%) and JNK (91–101%) between test compound-treated and untreated control (p>0.05).

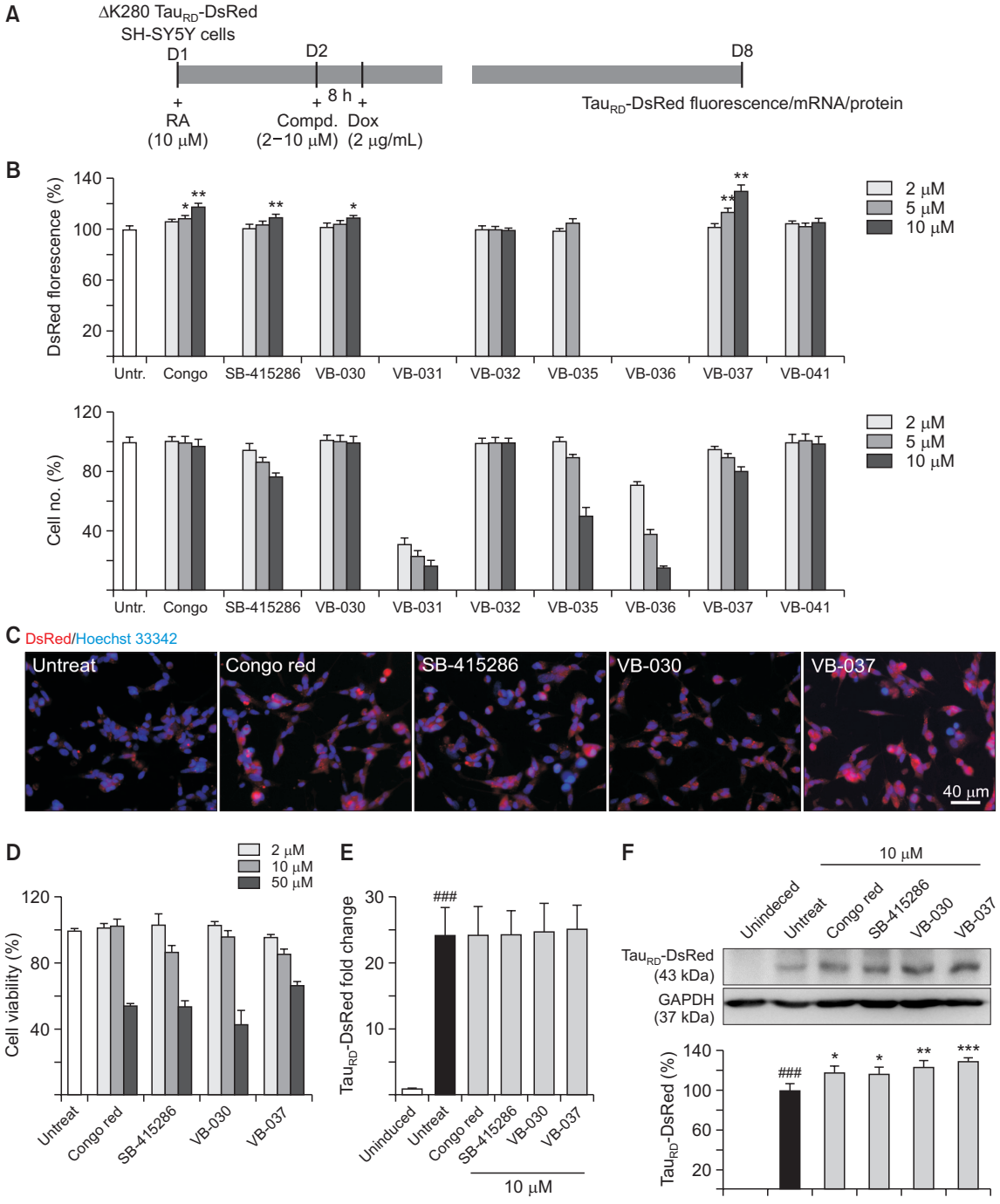

Fig. 2. VB compounds screen using the Tet-On ΔK280 TauRD-DsRed SH-SY5Y cell model for AD. (A) Experimental flowchart. On day 1, cells were plated with retinoic acid (RA, 10 μM) added to the culture medium. On day 2, congo red, SB-415286 or VB compounds (2–10 μM) was added to the cells for 8 h, followed by inducing ΔK280 TauRD-DsRed expression with doxycycline (Dox, 2 μg/mL) for 6 days. On day 8, DsRed fluorescence, TauRD-DsRed RNA and soluble TauRD-DsRed protein were measured. (B) Assessment of DsRed fluorescence with test compounds treatment (n=3). The relative DsRed fluorescence of untreated cells (Untr.) was normalized as 100%. *p* values: comparisons between with and without compound addition (**p*<0.05, ***p*<0.01; two-tailed Student's t test). Shown below were cell number analyzed in each treatment. (C) Fluorescent images of ΔK280 TauRD-DsRed cells with or without congo red, SB-415286, VB-030 or VB-037 (10 μM) treatment. Nuclei were counterstained with Hoechst 33342 (blue). (D) Cytotoxicity of test compounds examined using the 3-(4,5-dimethylthiazol-2-yl)-2,5-diphenyltetrazolium bromide (MTT) assay. Cells were treated with test compound (2–50 μM) for cell viability measurement (n=3). To normalize, the relative viability of untreated cells was set at 100%. (E) TauRD-DsRed RNA and (F) soluble TauRD-DsRed protein in ΔK280 TauRD-DsRed-expressing cells untreated or treated with congo red, SB-415286, VB-030 or VB-037 at 10 μM (n=3). *p* values: comparisons between induced (Dox+) vs. uninduced (Dox-) cells ($^{###}p$<0.001), or compound-treated vs. untreated (both are under Dox+) cells (**p*<0.05, ***p*<0.01, ****p*<0.001; one-way ANOVA with a post hoc Tukey test).

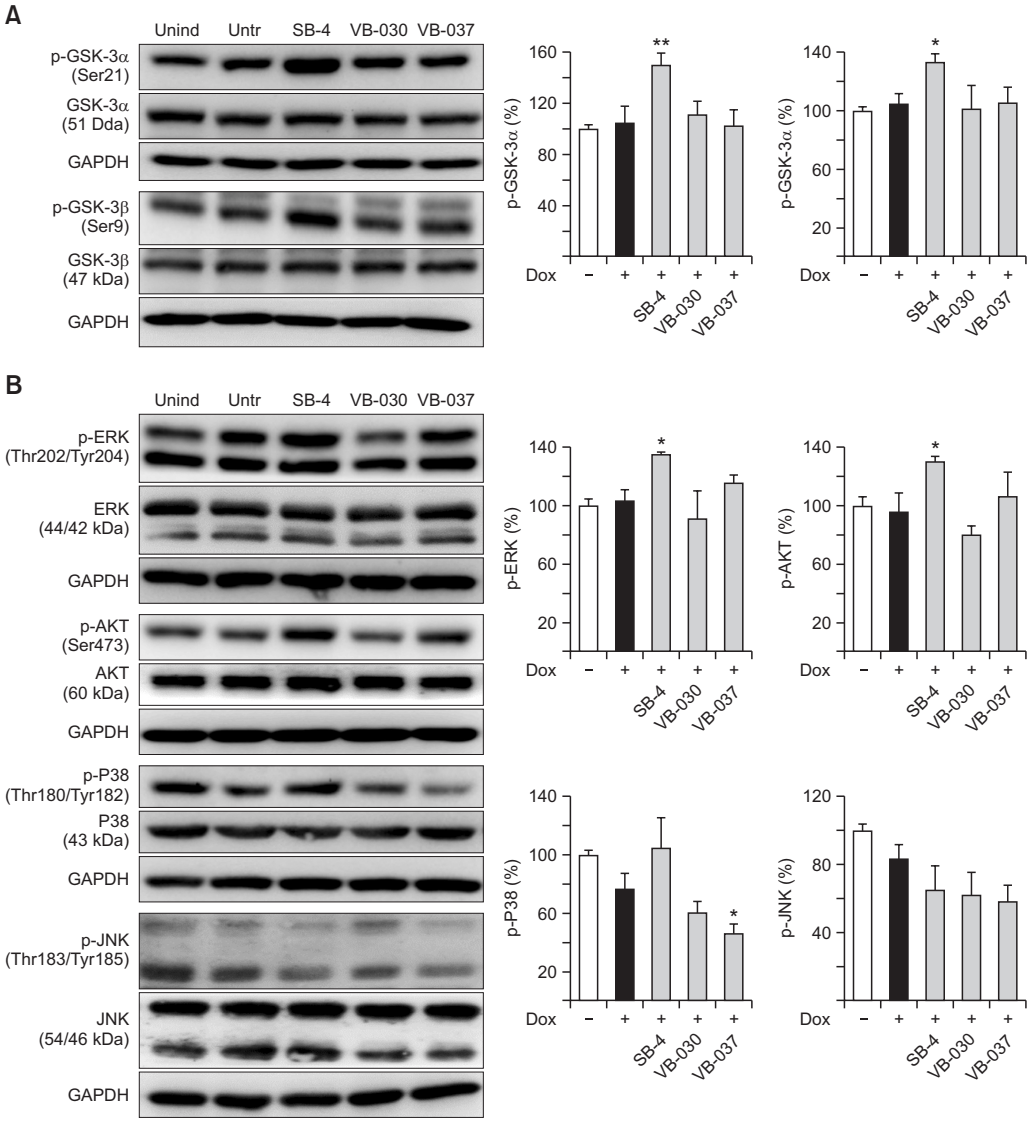

Fig. 3. Effects of VB-030 and VB-037 on GSK-3α, GSK-3β, ERK, AKT, P38, JNK and Tau phosphorylation in ΔK280 TauRD-DsRed SH-SY5Y cells. Western blot analysis of (A) GSK-3α (Ser21), GSK-3β (Ser9), (B) ERK (Thr202/Tyr204), AKT (Ser473), P38 (Thr180/Tyr182), JNK (Thr183/Tyr185), and (C) Tau (Ser202, Thr231, Ser396 and Ser404). GAPDH was used as a loading control (n=3). To normalize, the relative protein of uninduced cells was set at 100%. *p* values: comparisons between with and without doxycycline addition, or between with and without compound treatment (**p*<0.05, ***p*<0.01 and ****p*<0.001) (one-way ANOVA with a post hoc Tukey test).

We then examined whether SB-415286, VB-030 or VB-037 treatment could inhibit endogenous Tau phosphorylation at Ser202, Thr231, Ser396 and Ser404 in ΔK280 Tau_{RD}-DsRed-expressing SH-SY5Y cells. As shown in Fig. 3C, the steady-state levels of total Tau showed no significant difference between test compound-treated and untreated cells (100-106% versus 100%, $p>0.05$). However, the levels of p-Tau in SB-415286, VB-030 or VB-037 compound-treated cells were significantly reduced to 60-29% at Ser202 ($p=0.011-<0.001$), to 73-27% at Thr231 ($p=0.004-<0.001$), to 76–57% at Ser396 ($p=0.038-0.001$), and to 55-34% at Ser404 ($p=0.017-<0.001$), respectively, compared with untreated cells (100%). Collectively, these results suggest that resembling SB-415286, the two VB compounds inhibit Tau phosphorylation in ΔK280 Tau_{RD}-DsRed SH-SY5Y cells.

Tests of VB compounds on mouse hippocampal primary neuron culture

To evaluate whether compounds VB-030 and VB-037 are with neuroprotective activity, we further applied 10 μM compounds to mouse hippocampal primary culture under Tau toxicity, given that both compounds at 10 μM reduced Tau protein aggregation in SH-SY5Y cells. It has been reported that co-treatment of wortmannin (WT) (inhibitor of PI3K) and GF109203X (GFX) (inhibitor of PKC) increased GSK-3 activity and decreased cell viability (Xu *et al*., 2005). Therefore, we tested VB compounds on mouse hippocampal primary culture treated with WT and GFX to intensely activated GSK-3 and enhanced Tau hyperphosphorylation. The neuronal survival and neurite morphology were analyzed by immunocytochemical staining. In vehicle control groups, the neurite length ranged

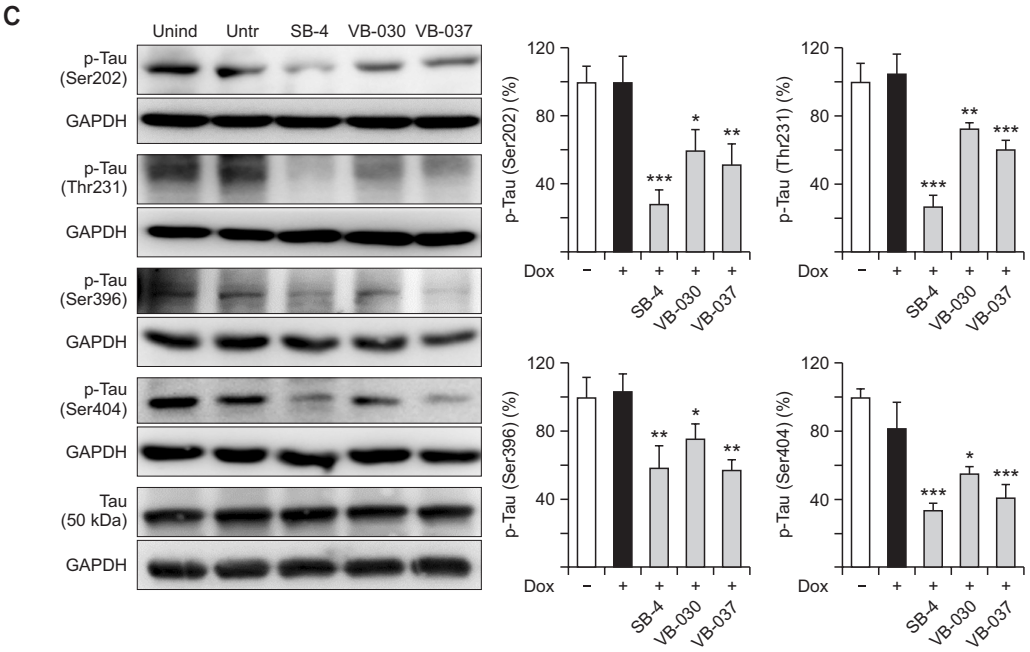

Fig. 3. Continued.

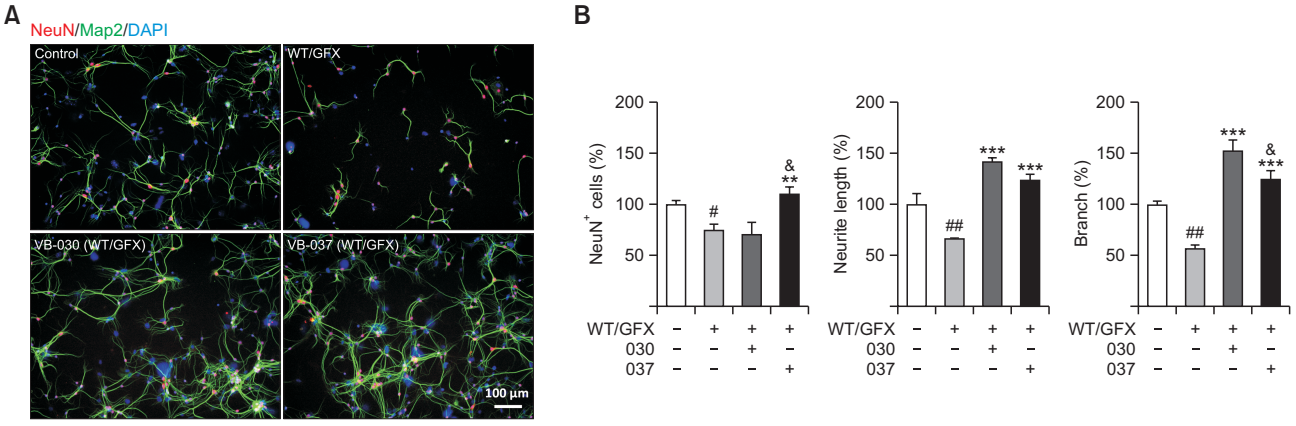

Fig. 4. Effect of VB-030 and VB-037 on mouse hippocampal primary culture under Tau toxicity. (A) The representative immunocytochemical image of cultures. Red, green and blue were staining of NeuN, Map2 and DAPI, respectively. (B) The quantitative results of neuronal survival and neurite morphology from immunocytochemical images (n=3). For normalization, the levels of vehicle-treated cells (control) were set as 100%. *p* values between WT+GFX-treated versus vehicle-treated ($^{\#}$), VB-030 or VB-037-treated versus untreated (*), or VB-030-treated versus VB-037-treated (&) were compared. $^{\#}$ and &: $p<0.05$, $^{\#\#}$ and **: $p<0.01$, ***: $p<0.001$ (one-way ANOVA with a post hoc Tukey test).

250-300 μm and the number of branches ranged 15-20; while in WT/GFX group, the neurite length ranged 180-200 μm and the number of branches ranged 8-10. The representative staining images are shown in Fig. 4A. The WT and GFX treatment significantly reduced the neuronal survival (p=0.045), neurite length (p=0.006) and branching (p=0.003) (Fig. 4B). VB-037 has significant protective effect for neuronal survival (p=0.009). Both VB-030 and VB-037 significantly increased the neurite length (p<0.001) and branching (p<0.001). Although VB-030 is not effective as VB-037 in neuronal survival, however, its activity in promoting neurite branching (p=0.022) is significantly better than VB-037 (Fig. 4B).

DISCUSSION

Effective treatments to slow AD neurodegeneration are still unavailable. GSK-3β, a key player in AD pathophysiology, influences all the major hallmarks of the disease including: amyloid-β production, Tau phosphorylation, memory formation and storage, neuronal growth, and synaptic plasticity (Lauretti *et al*., 2020). The expanding role of GSK-3β inhibitor suggests GSK-3β, a valuable therapeutic target for AD. In the present study, virtual screening was first performed on compounds from an Enamine's compound database using structure-based docking computation. This yielded 7 potential compounds which exerted inhibition in the GSK-3β enzyme assay.

We then used human SH-SY5Y cells expressing pro-aggregator Tau as a platform to identify two quinoline compounds VB-030 and VB-037 as Tau aggregate reducers. Through inhibiting GSK-3β kinase activity or p-P38 (Thr180/Tyr182), both compounds reduced endogenous Tau phosphorylation at Ser202, Thr231, Ser396 and Ser404 in neuronally differentiated SH-SY5Y cells expressing ΔK280 Tau_{RD}. Furthermore, both compounds displayed neuroprotective activity on mouse hippocampal primary culture under Tau cytotoxicity (Fig. 4).

Similar to the previously described mouse N2a ΔK280 Tau_{RD} cell model (Khlistunova *et al*., 2006), our human SH-SY5Y cell model was readily used to develop hits that prevent Tau aggregation in cells. In addition to reducing ΔK280 Tau_{RD}-DsRed aggregation, VB-030 and VB-037 also reduced Aβ aggregation in both thioflavin T biochemical assay and Aβ-green fluorescent protein (GFP)-expressing HEK293 AD cell model (Chiu *et al*., 2019). Whether the possible chemical chaperone activity of VB-030 and VB-037 contributes to the folding and/or stability of pro-aggregant Tau remains to be determined.

Tau phosphorylation is regulated by a balance between Tau kinase and phosphatase activities. In the case where the high number of Tau phosphorylation sites is involved in AD, GSK-3β is a promising target involved with 70% pathological Tau phosphorylation sites (Martin *et al*., 2013). GSK-3β phosphorylates predominantly Ser/Thr-Pro motifs in Tau protein including Ser202, Thr231, Ser396 and Ser400 (Li and Paudel, 2006). Studies of *in vitro* phosphorylation assay and NMR spectroscopy reveal that Tau residues Ser-396, Ser-400 and Ser-404 can be phosphorylated by GSK3β alone, and Ser-404 is essential in this process, as its mutation to Ala prevents all activity of GSK3β (Leroy *et al*., 2010). Phosphorylation of Thr231 by GSK-3β plays an important role in Tau's hyperphosphorylation and functional regulation (Lin *et al*., 2007). Although mammals have distinct genes encoding GSK-3 α and β isoforms which share amino acid sequence identity of 97% within their kinase domains (Woodgett, 1990), gene knockout experiments in mice revealed that Thr231/Thr235 and Ser396 on Tau proteins are phosphorylated predominantly by GSK-3β isoform (Soutar *et al*., 2010). At 0.018 μM concentration, residual GSK-3β activities were 36.1% for VB-030 and 90.9% for VB-037 (Table 2), not reflecting the level of inactive pGSK-3β (Ser9) in cells treated with 10 μM VB-030 (102%) or VB-037 (106%) (Fig. 3A). In addition, stronger inhibition of Tau phosphorylation at Ser202 (52% versus 60%), Thr231 (61% versus 73%), Ser396 (57% versus 76%) and Ser404 (42% versus 55%) was seen with VB-037 compared to VB-030 (Fig. 3C), although not significant. VB-037 has been reported to reduce the phosphor/total ratio of P38 in lipopolysaccharide/interferon-γ-inflamed Aβ-GFP-expressing SH-SY5Y AD cell model (Chiu *et al*., 2019). The lack of negative correlation between the observed Tau Ser202, Thr231, Ser396 and Ser404 phosphorylation and GSK-3β Ser9 phosphorylation in VB-030/037-treated cells indicates that P38 kinase regulating Tau phosphorylation at these sites may also be affected by

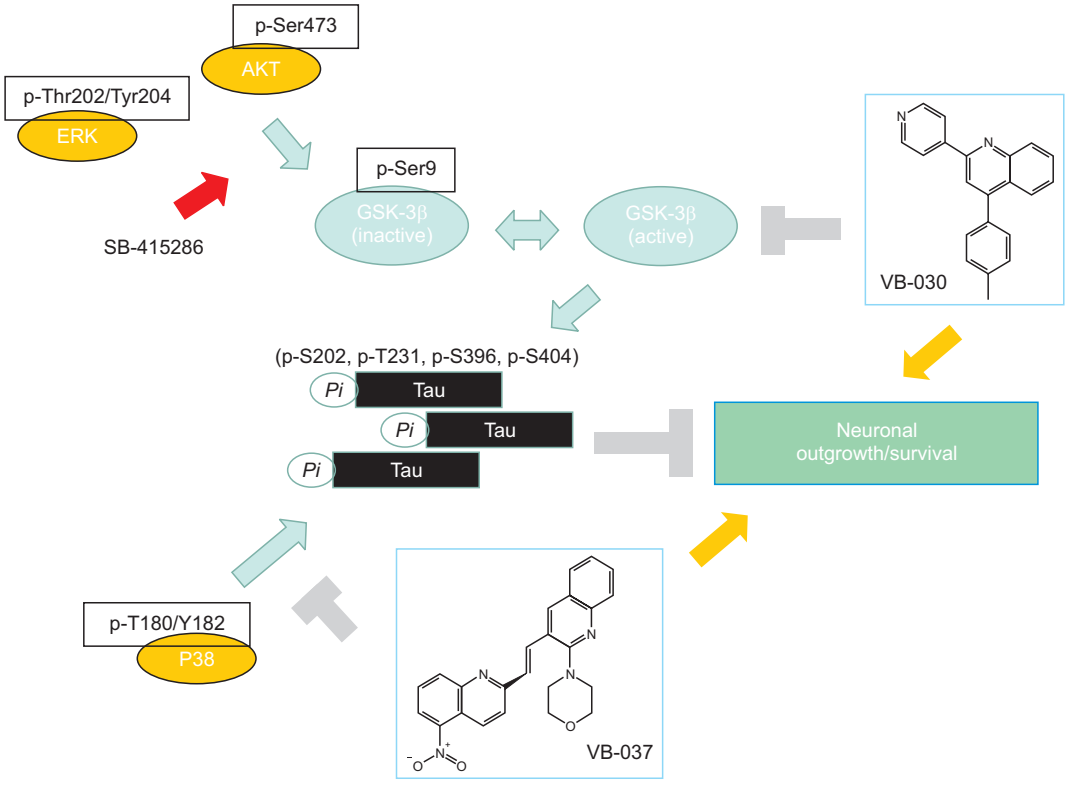

Fig. 5. Model for Tau aggregation reduction and neuronal outgrowth/survival promotion by quinoline compounds VB-030 and VB-037 in AD cell model. The known GSK-3 inhibitor SB-415286 increases the level of p-ERK (Thr202/Tyr204) and p-AKT (Ser473) to increase inactive p-GSK-3β (Ser9), while the tested VB-030 and VB-037 inhibit active GSK-3β and p-P38 (Thr180/Tyr182) respectively, to reduce endogenous Tau phosphorylation at Ser202, Thr231, Ser396 and Ser404 in SH-SY5Y cells, and improved neuronal survival and/or neurite length and branch in mouse hippocampal primary culture under Tau cytotoxicity.

VB-037 in ΔK280 Tau_{RD}-DsRed-expressing SH-SY5Y cells.

Through coordinating multiple proliferation and differentiation signals, GSK-3 is a master regulator of neural progenitor homeostasis (Kim *et al*., 2009). In addition, there are many studies about the association of GSK-3β and β-catenin in AD pathogenesis. Active GSK-3β has been found in brains staged for AD neurofibrillary changes (Pei *et al*., 1999), and β-catenin levels are reduced in AD patients (Zhang *et al*., 1998). Overexpression of GSK-3β in mice causes impairment in spatial learning (Hernandez *et al*., 2002). Over-activated GSK-3β can downregulate the efficiency of the PS1/N-cadherin/β-catenin complex causing deficiencies in synaptic and neuronal viability that leads to AD pathology (Uemura *et al*., 2007). Therefore, GSK-3β inhibitors stabilize β-catenin, which presents at synaptic terminals associates with the cytoplasmic domain of cadherin and regulate cell adhesion and influence synaptic size and strength (Murase *et al*., 2002; Maguschak and Ressler, 2008).

Increasing evidences have suggested that GSK-3β activation-mediated hyperphosphorylation of Tau can induce neuronal apoptosis (Gao *et al*., 2014; Jiang *et al*., 2016). Inhibition of GSK-3β by lithium treatment reduced Tau phosphorylation and improved cognitive deficits in animal models of AD (Fiorentini *et al*., 2010). The progressive cognitive decline and memory loss are strongly associated with neurite outgrowth and synaptic plasticity, which are early and invariant features of AD (Scheff *et al*., 2007). Compelling evidence also showed that GSK-3β inhibitor could promote neurite outgrowth in SH-SY5Y cells (Lin *et al*., 2016) and APP/PS1 transgenic mice (Long *et al*., 2015). Our study showed both VB-030 and VB-037 could benefit the neurite outgrowth against the Tau toxicity in mouse hippocampal primary neurons (Fig. 4), and their effect in reduction of Tau hyperphosphorylation was proved in SH-SY5Y cells (Fig. 3). We suggest the VB-030 and VB-037 are two potent Tau hyperphosphorylation inhibitors with neuroprotective effect for tauopathy, including AD.

Both VB-030 and VB-037 are nitrogen-containing heterocyclic aromatic compounds with quinoline scaffold. Biologically active quinoline derivatives possessing dual effects of inhibition of Aβ toxicity in MC65 neuroblastoma cells and GSK-3β enzyme have been documented (Lu *et al*., 2014). In our study, quinoline derivatives VB-030 and VB-037 display protective activity against Tau toxicity in mouse hippocampal primary neurons (Fig. 4) and enzymatic inhibitory activity against GSK-3β (Table 2), reinforcing the development of quinoline analogs as anti-AD agents.

In addition to quinoline scaffold, VB-037 also contains a heterocycle morpholine moiety featuring both amine and ether functional groups. Morpholine-containing compounds with potent *in vitro* GSK-3β inhibitory activity and *in vivo* Tau phosphorylation inhibitory activity have been addressed (Fukunaga *et al*., 2013). The potency of VB-037 may be improved by introducing a small alkyl group to the 3-position of the morpholine moiety (Fukunaga *et al*., 2015). Further development of VB-037 analogs and test of *in vivo* Tau phosphorylation inhibitory activity are warranted.

In summary, through combinations of virtual screening, GSK-3β enzyme assay, and models of human SH-SY5Y cells expressing Tau folding reporter and mouse hippocampal primary neuron culture under Tau cytotoxicity, two quinoline compounds VB-030 and VB-037 were identified and experimental results showed that they effectively inhibit GSK-3β kinase activity or p-P38 (Thr180/Tyr182) (Fig. 5). Further study will be needed to confirm that this also works in AD animal models and eventually humans.

CONFLICT OF INTEREST

All authors have no conflicts of interest to declare.

ACKNOWLEDGMENTS

We thank the Molecular Imaging Core Facility of National Taiwan Normal University for the technical assistance. This work was supported by the grants 103-2321-B-182-008, 103-2321-B-003-003, 104-2325-B-003-001 and 104-2325-B-003-003 from the Ministry of Science and Technology, and 104T3040B05 and 104T3040B07 from National Taiwan Normal University, Taipei, Taiwan.

REFERENCES

Alabed, Y. Z., Pool, M., Ong Tone, S., Sutherland, C. and Fournier, A. E. (2010) GSK3β regulates myelin-dependent axon outgrowth inhibition through CRMP4. *J. Neurosci.* **30**, 5635-5643.

Chiu, Y. J., Hsieh, Y. H., Lin, T. H., Lee, G. C., Hsieh-Li, H. M., Sun, Y. C., Chen, C. M., Chang, K. H. and Lee-Chen, G. J. (2019) Novel compound VB-037 inhibits Aβ aggregation and promotes neurite outgrowth through enhancement of HSP27 and reduction of P38 and JNK-mediated inflammation in cell models for Alzheimer's disease. *Neurochem. Int.* **125**, 175-186.

Croft, C. L., Kurbatskaya, K., Hanger, D. P. and Noble, W. (2017) Inhibition of glycogen synthase kinase-3 by BTA-EG4 reduces tau abnormalities in an organotypic brain slice culture model of Alzheimer's disease. *Sci. Rep.* **7**, 7434.

Cross, D. A., Alessi, D. R., Cohen, P., Andjelkovich, M. and Hemmings, B. A. (1995) Inhibition of glycogen synthase kinase-3 by insulin mediated by protein kinase B. *Nature* **378**, 785-789.

Cross, D. A., Culbert, A. A., Chalmers, K. A., Facci, L., Skaper, S. D. and Reith, A. D. (2001) Selective small-molecule inhibitors of glycogen synthase kinase-3 activity protect primary neurones from death. *J. Neurochem.* **77**, 94-102.

del Ser, T., Steinwachs, K. C., Gertz, H. J., Andres, M. V., Gomez-Carrillo, B., Medina, M., Vericat, J. A., Redondo, P., Fleet, D. and Leon, T. (2013) Treatment of Alzheimer's disease with the GSK-3 inhibitor tideglusib: a pilot study. *J. Alzheimers Dis.* **33**, 205-215.

Eldar-Finkelman, H. and Martinez, A. (2011) GSK-3 Inhibitors: preclinical and clinical focus on CNS. *Front. Mol. Neurosci.* **4**, 32.

Fiorentini, A., Rosi, M. C., Grossi, C., Luccarini, I. and Casamenti, F. (2010) Lithium improves hippocampal neurogenesis, neuropathology and cognitive functions in APP mutant mice. *PLoS ONE* **5**, e14382.

Fukunaga, K., Sakai, D., Watanabe, K., Nakayama, K., Kohara, T., Tanaka, H., Sunada, S., Nabeno, M., Okamoto, M., Saito, K.I., Eguchi, J. I., Mori, A., Tanaka, S., Inazawa, K. and Horikawa, T. (2015) Discovery of novel 2-(alkylmorpholin-4-yl)-6-(3-fluoropyridin-4-yl)-pyrimidin-4(3H)-ones as orally-active GSK-3β inhibitors for Alzheimer's disease. *Bioorg. Med. Chem. Lett.* **25**, 1086-1091.

Fukunaga, K., Uehara, F., Aritomo, K., Shoda, A., Hiki, S., Okuyama, M., Usui, Y., Watanabe, K., Yamakoshi, K., Kohara, T., Hanano, T., Tanaka, H., Tsuchiya, S., Sunada, S., Saito, K. I., Eguchi, J. I., Yuki, S., Asano, S., Tanaka, S., Mori, A., Yamagami, K., Baba, H., Horikawa, T. and Fujimura, M. (2013) 2-(2-Phenylmorpholin-4-yl) pyrimidin-4(3H)-ones, a new class of potent, selective and orally active glycogen synthase kinase-3β inhibitors. *Bioorg. Med. Chem. Lett.* **23**, 6933-6937.

Gao, C., Liu, Y., Jiang, Y., Ding, J. and Li, L. (2014) Geniposide ame-

liorates learning memory deficits, reduces tau phosphorylation and decreases apoptosis via GSK3β pathway in streptozotocin-induced alzheimer rat model. *Brain Pathol.* **24**, 261-269.

Grimes, C. A. and Jope, R. S. (2001) The multifaceted roles of glycogen synthase kinase 3β in cellular signaling. *Prog. Neurobiol.* **65**, 391-426.

Hampel, H., Ewers, M., Burger, K., Annas, P., Mortberg, A., Bogstedt, A., Frolich, L., Schroder, J., Schonknecht, P., Riepe, M. W., Kraft, I., Gasser, T., Leyhe, T., Möller, H. J., Kurz, A. and Basun, H. (2009) Lithium trial in Alzheimer's disease: a randomized, single-blind, placebo-controlled, multicenter 10-week study. *J. Clin. Psychiatry* **70**, 922-931.

Hardy, J. (2006) A hundred years of Alzheimer's disease research. *Neuron* **52**, 3-13.

Hernandez, F., Borrell, J., Guaza, C., Avila, J. and Lucas, J. J. (2002) Spatial learning deficit in transgenic mice that conditionally overexpress GSK-3beta in the brain but do not form tau filaments. *J. Neurochem.* **83**, 1529-1533.

Hitchcock, S. A. and Pennington, L. D. (2006) Structure - brain exposure relationships. *J. Med. Chem.* **49**, 7559-7583.

Hur, E. M. and Zhou, F. Q. (2010) GSK3 signalling in neural development. *Nat. Rev. Neurosci.* **11**, 539-551.

Inbar, P., Li, C. Q., Takayama, S. A., Bautista, M. R. and Yang, J. (2006) Oligo(ethylene glycol) derivatives of thioflavin T as inhibitors of protein-amyloid interactions. *ChemBioChem* **7**, 1563-1566.

Jiang, W., Luo, T., Li, S., Zhou, Y., Shen, X. Y., He, F., Xu, J. and Wang, H. Q. (2016) Quercetin protects against Okadaic acid-induced injury via MAPK and PI3K/Akt/GSK3β signaling pathways in HT22 hippocampal neurons. *PLoS ONE* **11**, e0152371.

Khlistunova, I., Biernat, J., Wang, Y., Pickhardt, M., von Bergen, M., Gazova, Z., Mandelkow, E. and Mandelkow, E. M. (2006) Inducible expression of Tau repeat domain in cell models of tauopathy: aggregation is toxic to cells but can be reversed by inhibitor drugs. *J. Biol. Chem.* **281**, 1205-1214.

Kim, W. Y., Wang, X., Wu, Y., Doble, B. W., Patel, S., Woodgett, J. R. and Snider. W. D. (2009) GSK-3 is a master regulator of neural progenitor homeostasis. *Nat. Neurosci.* **12**, 1390-1397.

Lauretti, E. and Praticò, D. (2015) Glucose deprivation increases tau phosphorylation via P38 mitogen-activated protein kinase. *Aging Cell* **14**, 1067-1074.

Lauretti, E., Dincer, O. and Praticò, D. (2020) Glycogen synthase kinase-3 signaling in Alzheimer's disease. *Biochim. Biophys. Acta Mol. Cell Res.* **1867**, 118664.

Lee, C. W., Lau, K. F., Miller, C. C. and Shaw, P. C. (2003) Glycogen synthase kinase-3β-mediated tau phosphorylation in cultured cell lines. *Neuroreport* **14**, 257-260.

Leroy, A., Landrieu, I., Huvent, I., Legrand, D., Codeville, B., Wieruszeski, J. M. and Lippens, G. (2010) Spectroscopic studies of GSK3β phosphorylation of the neuronal tau protein and its interaction with the N-terminal domain of apolipoprotein E. *J. Biol. Chem.* **285**, 33435-33444.

Leyhe, T., Eschweiler, G. W., Stransky, E., Gasser, T., Annas, P., Basun, H. and Laske, C. (2009) Increase of BDNF serum concentration in lithium treated patients with early Alzheimer's disease. *J. Alzheimers Dis.* **16**, 649-656.

Li, M., Wang, X., Meintzer, M. K., Laessig, T., Birnbaum, M. J. and Heidenreich, K. A. (2000) Cyclic AMP promotes neuronal survival by phosphorylation of glycogen synthase kinase 3β. *Mol. Cell. Biol.* **20**, 9356-9363.

Li, T. and Paudel, H. K. (2006) Glycogen synthase kinase 3β phosphorylates Alzheimer's disease-specific Ser396 of microtubule-associated protein tau by a sequential mechanism. *Biochemistry* **45**, 3125-3133.

Lin, C. H., Hsieh, Y. S., Wu, Y. R., Hsu, C. J., Chen, H. C., Huang, W. H., Chang, K. H., Hsieh-Li, H. M., Su, M. T., Sun, Y. C., Lee G. C. and Lee-Chen, G. J. (2016) Identifying GSK-3β kinase inhibitors of Alzheimer's disease: virtual screening, enzyme, and cell assays. *Eur. J. Pharm. Sci.* **89**, 11-19.

Lin, Y. T., Cheng, J. T., Liang, L. C., Ko, C. Y., Lo, Y. K. and Lu, P. J. (2007) The binding and phosphorylation of Thr231 is critical for Tau's hyperphosphorylation and functional regulation by glycogen synthase kinase 3β. *J. Neurochem.* **103**, 802-813.

Lipinski, C. A., Lombardo, F., Dominy, B. W. and Feeney, D. P. (2001) Experimental and computational approaches to estimate solubility and permeability in drug discovery and development settings. *Adv. Drug Deliv. Rev.* **46**, 3-26.

Liu, H., Wang, L., Lv, M., Pei, R., Li, P., Pei, Z., Wang, Y., Su, W. and Xie, X. Q. (2014) AlzPlatform: an Alzheimer's disease domain-specific chemogenomics knowledgebase for polypharmacology and target identification research. *J. Chem. Inf. Model.* **54**, 1050-1060.

Liu, S. J., Zhang, A. H., Li, H. L., Wang, Q., Deng, H. M., Netzer, W. J., Xu, H. and Wang, J. Z. (2003) Overactivation of glycogen synthase kinase-3 by inhibition of phosphoinositol-3 kinase and protein kinase C leads to hyperphosphorylation of tau and impairment of spatial memory. *J. Neurochem.* **87**, 1333-1344.

Long, Z. M., Zhao, L., Jiang, R., Wang, K. J., Luo, S. F., Zheng, M., Li, X. F. and He, G. Q. (2015) Valproic acid modifies synaptic structure and accelerates neurite outgrowth via the glycogen synthase kinase-3β signaling pathway in an Alzheimer's disease model. *CNS Neurosci. Ther.* **21**, 887-897.

Lovestone, S., Boada, M., Dubois, B., Hull, M., Rinne, J. O., Huppertz, H. J., Calero, M., Andres, M. V., Gomez-Carrillo, B., Leon, T. and del Ser, T.; ARGO investigators (2015) A phase II trial of tideglusib in Alzheimer's disease. *J. Alzheimers Dis.* **45**, 75-88.

Lu, J., Maezawa, I., Weerasekara, S., Erenler, R., Nguyen, T. D. T., Nguyen, J., Swisher, L. Z., Li, J., Jin, L. W., Ranjan, A., Srivastava, S. K. and Hua, D. H. (2014) Syntheses, neural protective activities, and inhibition of glycogen synthase kinase-3β of substituted quinolines. *Bioorg. Med. Chem. Lett.* **24**, 3392-3397.

Lucas, J. J., Hernandez, F., Gomez-Ramos, P., Moran, M. A., Hen, R. and Avila, J. (2001) Decreased nuclear β-catenin, tau hyperphosphorylation and neurodegeneration in GSK-3β conditional transgenic mice. *EMBO J.* **20**, 27-39.

Maguschak, K. A. and Ressler, K. J. (2008) β-catenin is required for memory consolidation. *Nat. Neurosci.* **11**, 1319-1326.

Martin, L., Latypova, X., Wilson, C. M., Magnaudeix, A., Perrin, M. L., Yardin, C. and Terro, F. (2013) Tau protein kinases: involvement in Alzheimer's disease. *Ageing Res. Rev.* **12**, 289-309.

Murase, S., Mosser, E. and Schuman, E. M. (2002) Depolarization drives β-catenin into neuronal spines promoting changes in synaptic structure and function. *Neuron* **35**, 91-105.

Nemoto, T., Miyazaki, S., Kanai, T., Maruta, T., Satoh, S., Yoshikawa, N., Yanagita, T. and Wada, A. (2010) Nav1.7-Ca^{2+} influx-induced increased phosphorylations of extracellular signal-regulated kinase (ERK) and p38 attenuate tau phosphorylation via glycogen synthase kinase-3beta: priming of Nav1.7 gating by ERK and p38. *Eur. J. Pharmacol.* **640**, 20-28.

Noble, W., Planel, E., Zehr, C., Olm, V., Meyerson, J., Suleman, F., Gaynor, K., Wang, L., LaFrancois, J., Feinstein, B., Burns, M., Krishnamurthy, P., Wen, Y., Bhat, R., Lewis, J., Dickson, D. and Duff, K. (2005) Inhibition of glycogen synthase kinase-3 by lithium correlates with reduced tauopathy and degeneration *in vivo*. *Proc. Natl. Acad. Sci. U.S.A.* **102**, 6990-6995.

Pei, J. J., Tanaka, T., Tung, Y. C., Braak, E., Iqbal, K. and Grundke-Iqbal, I. (1997) Distribution, levels, and activity of glycogen synthase kinase-3 in the Alzheimer disease brain. *J. Neuropathol. Exp. Neurol.* **56**, 70-78.

Pei, J. J., Braak, E., Braak, H., Grundke-Iqbal, I., Iqbal, K., Winblad, B. and Cowburn, R. F. (1999) Distribution of active glycogen synthase kinase 3β (GSK-3β) in brains staged for Alzheimer disease neurofibrillary changes. *J. Neuropathol. Exp. Neurol.* **58**, 1010-1019.

Perola, E. (2006) Minimizing false positives in kinase virtual screens. *Proteins* **64**, 422-435.

Ploia, C., Antoniou, X., Sclip, A., Grande, V., Cardinetti, D., Colombo, A., Canu, N., Benussi, L., Ghidoni, R., Forloni, G. and Borsello, T. (2011) JNK plays a key role in tau hyperphosphorylation in Alzheimer's disease models. *J. Alzheimers Dis.* **26**, 315-329.

Scheff, S. W., Price, D. A., Schmitt, F. A., DeKosky, S. T. and Mufson, E. J. (2007) Synaptic alterations in CA1 in mild Alzheimer disease and mild cognitive impairment. *Neurology* **68**, 1501-1508.

Seira, O., Gavin, R., Gil, V., Llorens, F., Rangel, A., Soriano, E. and del Rio, J. A. (2010) Neurites regrowth of cortical neurons by GSK3β inhibition independently of Nogo receptor 1. *J. Neurochem.* **113**, 1644-1658.

Shi, X. L., Yan, N., Cui, Y. J. and Liu, Z. P. (2020) A unique GSK-3β inhibitor B10 has a direct effect on Aβ, targets Tau and metal dyshomeostasis, and promotes neuronal neurite outgrowth. *Cells* **9**, 649.

Soutar, M. P., Kim, W. Y., Williamson, R., Peggie, M., Hastie, C. J., McLauchlan, H., Snider, W. D., Gordon-Weeks, P. R. and Sutherland, C. (2010) Evidence that glycogen synthase kinase-3 isoforms have distinct substrate preference in the brain. *J. Neurochem.* **115**, 974-983.

Su, Y., Ryder, J., Li, B., Wu, X., Fox, N., Solenberg, P., Brune, K., Paul, S., Zhou, Y., Liu, F. and Ni, B. (2004) Lithium, a common drug for bipolar disorder treatment, regulates amyloid-β precursor protein processing. *Biochemistry* **43**, 6899-6908.

Uemura, K., Kuzuya, A., Shimozono, Y., Aoyagi, N., Ando, K., Shimohama, S. and Kinoshita, A. (2007) GSK3βactivity modifies the localization and function of presenilin. *J. Biol. Chem.* **282**, 15823-15832.

Verdonk, M. L., Cole, J. C., Hartshorn, M. J., Murray, C. W. and Taylor, R. D. (2003) Improved protein-ligand docking using GOLD. *Proteins* **52**, 609-623.

Woodgett, J. R. (1990) Molecular cloning and expression of glycogen synthase kinase-3/factor A. *EMBO J.* **9**, 2431-2438.

Xu, G. G., Deng, Y. Q., Liu, S. J., Li, H. L. and Wang, J. Z. (2005) Prolonged Alzheimer-like tau hyperphosphorylation induced by simultaneous inhibition of phosphoinositol-3 kinase and protein kinase C in N2a cells. *Acta Biochim. Biophys. Sin.* **37**, 349-354.

Xu, M., Wang, S. L., Zhu, L., Wu, P. Y., Dai, W. B. and Rakesh, K. P. (2019) Structure-activity relationship (SAR) studies of synthetic glycogen synthase kinase-3β inhibitors: a critical review. *Eur. J. Med. Chem.* **164**, 448-470.

Zhang, Z., Hartmann, H., Do, V. M., Abramowski, D., Sturchler-Pierrat, C., Staufenbiel, M., Sommer, B., van de Wetering, M., Clevers, H., Saftig, P., De Strooper, B., He, X. and Yankner, B. A. (1998) Destabilization of β-catenin by mutations in presenilin-1 potentiates neuronal apoptosis. *Nature* **395**, 698-702.

Zhang, H. C., Bonaga, L. V. R., Ye, H., Derian, C. K., Damiano, B. P. and Maryanoff, B. E. (2007) Novel bis(indolyl)maleimide pyridinophanes that are potent, selective inhibitors of glycogen synthase kinase-3. *Bioorg. Med. Chem. Lett.* **17**, 2863-2868.